Supplementary material

Materials and methods

Cell line and mice

CMT167 mouse lung cancer cells were acquired from the European Collection of Authenticated Cell Cultures [ECACC] (Salisbury, Wiltshire, UK). *Mycoplasma* contamination was ruled out prior to use. Mice were purchased from Jiangsu Jicui Yaokang Biotechnology Co., Ltd. (Nanjing, Jiangsu, China).

COX-2 overexpression (COX-2 OE) in murine tumor cells was achieved through lentiviral transduction. The COX-2-overexpressing lentivirus was procured from Genechem Inc. (Shanghai, China) and viral particles were subsequently used to infect tumor cells according to the manufacturer's protocol.

Mouse models, treatment, and administration

A subcutaneous tumor model was generated by injecting 1.0×10^6 CMT167 cells (in 100 μL) into 6-week-old C57BL/6 mice. Tumor dimensions were recorded every 3–4 d using calipers to monitor growth. The anesthetized mice were irradiated with 8 Gy for 3 consecutive days. Celecoxib (30 mg/kg, HY-14398; MCE, Shanghai, China) was administered once daily by gavage 5 days per week. Anti-PD-1 antibody (200 μg/mouse; BioXcell, Beijing, China) was injected three times per week. For combination therapy, treatment was started on the same day. All animal experiments were approved by the institutional Ethics Committee (SDTHEC202502219) and all procedures followed relevant ethical guidelines.

Cytokine ELISA analysis

Tumor tissues were collected from mice. The spleen tissue samples were homogenized in PBS using a tissue homogenizer. Then, the samples were centrifuged to obtain a homogenized tissue supernatant. The concentration of PGE2 was determined using a PGE2 kit (Elabscience, Wuhan, China) according to the manufacturer's instructions.

Flow cytometry

Subcutaneous tumors were harvested from mice and minced into small fragments using ophthalmic forceps at the end of the experimental period. The tissues were then digested in a solution containing 1 mg/mL of collagenase type IV (Thermo Fisher Scientific, Waltham, MA, USA) and 0.2 mg/mL of DNase I (Thermo Fisher Scientific, Waltham, MA, USA) for 30 min. The resulting cell suspension was filtered through a 70-μm cell strainer to obtain single cells. Cells were directly incubated with the appropriate fluorescent-conjugated antibodies for extracellular markers. Intracellular markers required a membrane permeabilization step prior to antibody staining. The antibody panel protocol for flow cytometry was as follows: BV605 anti-mouse CD45 (BD Biosciences, Franklin Lake, NJ, USA); FITC anti-mouse CD3 (BioLegend, Beijing, China); BV650 anti-mouse CD4 (BioLegend); AF700 anti-mouse CD8 (BioLegend); BV421 anti-mouse Ki-67 (BioLegend); PE anti-mouse GZMB (BD Biosciences); BV785 anti-mouse IFNγ (BioLegend); PE/Cy7 anti-mouse TNF-α (BioLegend); and AF647 anti-mouse TCF7/TCF1 (R&D Systems, Minneapolis, MN, USA).

Human tumor samples

Formalin-fixed, paraffin-embedded (FFPE) tumor specimens were obtained from 129 patients diagnosed with NSCLC at Shandong Cancer Hospital (Jinan, Shandong, China). Relevant clinical and pathologic data, including patient gender, age, cigarette smoking history, tumor size, and TNM classification, were retrieved from medical records. The retrospective analysis included 129 radioimmunotherapy-naive NSCLC patients enrolled between 2015 and 2016. The follow-up period ended on 31 September 2024. The median OS of the enrolled patients was 68 months. This investigation adhered to the principles outlined in the Declaration of Helsinki and received approval from the Ethics Committee of Shandong Cancer Hospital (SDTHEC2024002037). The study qualified for an exemption from informed consent due to its retrospective design, as formally authorized by the Ethics Committee.

Immunohistochemistry (IHC)

FFPE tissue sections were initially baked, then treated with a commercial dewaxing reagent, followed by stepwise rehydration in graded ethanol. Antigen retrieval was performed with ethylenediaminetetraacetic acid (EDTA) buffer (pH 6.0). After cooling to ambient temperature, endogenous peroxidase activity was blocked for 10–15 min and non-specific binding was subsequently suppressed for an additional 15 min. Sections were then incubated overnight at 4°C with a

primary antibody specific for COX-2 (12282; Cell Signaling Technology, Danfoss, MA, USA). After thorough rinsing the slides were developed using a DAB substrate, counterstained with hematoxylin, dehydrated, and sealed.

COX-2 expression was evaluated based on two parameters (the proportion of positively stained tumor cells and staining intensity). The percentage of positive cells was scored from 1–4, corresponding to 0%–25%, 26%–50%, 51%–75%, and 76%–100%, respectively. Staining intensity was rated on a 0–3 scale (none, weak, moderate, and strong, respectively). These two values were summed to yield a final score ranging from 0–8, with a total score ≥4 indicative of high COX-2 expression. All assessments were performed independently by a pathologist who was blinded to the clinical outcomes.

Multiplex immunofluorescence staining

FFPE sections (4 μm thick) were prepared according to the standard protocol described earlier. Antigen retrieval was performed using an appropriate buffer and sections were subsequently blocked for 1 h. Next, the slides were incubated with a cytokeratin [CK] antibody (ZM-0069; Beijing, China) at room temperature for 2 h, followed by an HRP-conjugated polymer and opal fluorophore using the OPAL 7-color IHC kit (Akoya Biosciences; Marlborough, MA, USA). After another round of antigen retrieval, the slides were sequentially probed with TCF1 (C63D9; CST), CD8 (D4W2Z; CST), and TOX antibodies (ab155768; Abcam, Cambridge, UK) with fluorophores applied after each incubation. Finally, the sections were counterstained with DAPI and mounted. Images were captured using a Vectra Polaris Quantitative Pathology Imaging System (Akoya Biosciences) and analyzed with InForm software (Akoya Biosciences).

Statistical analysis

GraphPad Prism and R software were used for all statistical evaluations. Statistical significance was defined as a $P < 0.05$. Associations between COX-2 or $CD8^+$ T cell infiltration and clinicopathologic features were examined using a chi-square test and Mantel–Haenszel trend test. The "Survminer" package was applied to determine a cut-off point for continuous variables, followed by patient stratification into high and low groups. Overall survival (OS) was estimated using the Kaplan–Meier method and comparisons between survival curves were performed with the log-rank test. Cox regression models identified independent prognostic indicators, adjusted for clinically relevant covariates, including TNM stage. For data presentation, means ± standard error of the mean (SEM) is shown. The difference between two groups was assessed using an unpaired two-tailed *t*-test. Differences between two groups were assessed using an unpaired two-tailed *t*-test. For comparisons involving multiple groups, one-way analysis of variance (ANOVA) was performed, followed by Tukey's multiple comparison test. The Benjamin-Hochberg false discovery rate correction was applied to account for multiple comparisons. A mixed-effects model was used to account for temporal effects and ensure accurate modeling of tumor growth data for the analysis of repeated measures data across multiple groups.

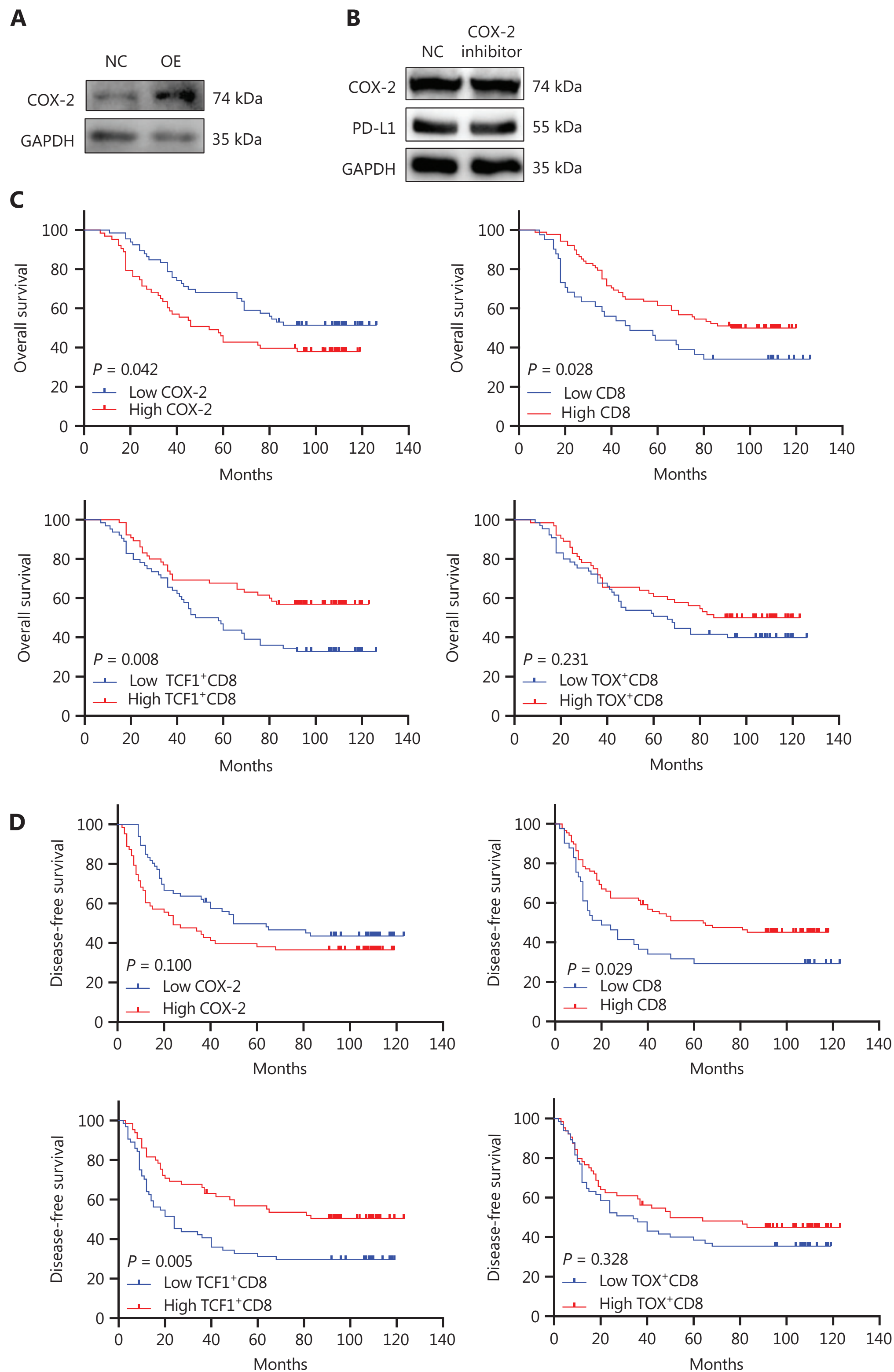

Figure S1 (A) The stable CMT-167 cell line overexpressing COX-2 was constructed. (B) Immunoblotting of PD-L1 in CMT-167 cells treated with COX-2 inhibitor. Dimethyl sulfoxide (DMSO) was used as negative control. (C, D) Kaplan–Meier survival analyses for patients with lung cancer.

Table S1 Correlation between clinicopathologic characteristics and stem-like $CD8^+$ T cells

Variables	$CD8^+T$		*P*	$TCF1^+CD8T$		*P*
	Low	High		Low	High	
Age						
<60	23	49	0.965	33	39	0.335
≥60	18	39		31	26	
Gender						
Male	16	48	0.101	30	34	0.537
Female	25	40		34	31	
Smoking history						
No	15	40	0.343	23	32	0.127
Yes	26	48		41	33	
TNM						
I	5	15	0.174	6	14	0.045
II	12	37		22	27	
III	24	36		36	24	
COX-2						
Low	16	50	0.060	27	39	0.043
High	25	38		37	26	

$P < 0.05$ is considered statistically significant.

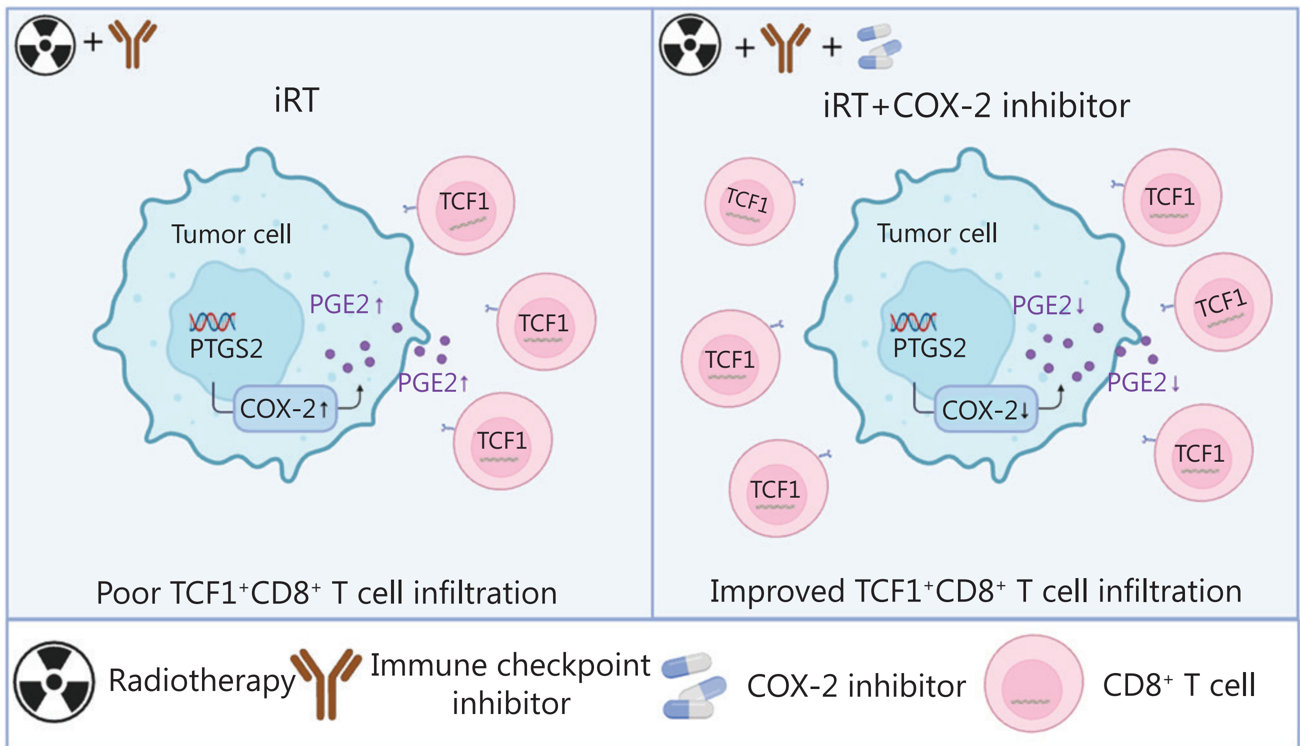

Figure S2 Scheme figure illustrates the effects of combining immune checkpoint inhibitors (iRTs) with COX-2 inhibitors in enhancing TCF1$^+$CD8$^+$ T cell infiltration in tumor cells.